Vol. 581: 215–227, 2017
https://doi.org/10.3354/meps12312

MARINE ECOLOGY PROGRESS SERIES
Mar Ecol Prog Ser

Published October 13

Marine predators and phytoplankton: how elephant seals use the recurrent Kerguelen plume

Malcolm O'Toole[1,*], Christophe Guinet[2], Mary-Anne Lea[1,3], Mark A. Hindell[1,3]

[1]Institute for Marine and Antarctic Studies, University of Tasmania, Hobart, TAS 7001, Australia
[2]Marine Predator Department, Centre d'études biologiques de Chizé, Villiers-en-Bois 79360, France
[3]Antarctic Climate and Ecosystems CRC, Hobart, TAS 7001, Australia

ABSTRACT: Predators feeding in a highly dynamic environment have evolved strategies to respond to patchy resource distribution. However, studying these ecological interactions is challenging in the marine environment, as both predators and elements in their environment are often highly mobile and difficult to monitor. We used sensors deployed on female southern elephant seals *Mirounga leonina* to collect data as they foraged hundreds of metres below a large recurrent phytoplankton plume east of the Kerguelen Islands (49° 15′ S, 69° 10′ E). Data collected by animal-borne light sensors were used to reconstruct phytoplankton patterns encountered by the seals. Prey encounter events (PEEs) recorded by seal-borne accelerometers below the euphotic zone were compared with phytoplankton estimates at 2 scales: mesoscale (10s to 100s km) and small scale (inter-dive). These analyses were performed on data recorded during daylight hours only, and did not include data at night due to the sensitivity threshold of the light sensors. Our results showed that elephant seals moved through alternating patches of high- and low-density phytoplankton, but the timing and locations of these bloom patches were different between the upper and lower euphotic layers. Seals recorded more PEEs and shallower dives below high-density patches of phytoplankton. We propose that phytoplankton density at the mesoscale facilitates prey aggregation (direct effect). However, phytoplankton density between dives (small scale) likely facilitates vertical access to prey via the shading effect of phytoplankton (indirect effect). Our study shows how a deep-diving marine predator may use its environment to maximise net energy intake, and we demonstrate its resilience in a highly dynamic ecosystem.

KEY WORDS: *Mirounga leonina* · Foraging strategy · Prey encounter events · Dive behaviour · Kerguelen phytoplankton plume · Prey access

Resale or republication not permitted without written consent of the publisher

INTRODUCTION

Phytoplankton is the basis of the marine food web, transferring energy to secondary producers like zooplankton, to mid-trophic level fish (Ware & Thomson 2005) and ultimately, to top predator birds and marine mammals. These primary resources tend to be patchily distributed in space and time, showing a clumped rather than a random or even distribution (d'Ovidio et al. 2010). In oligotrophic waters, where the surface mixed layer is depleted of nutrients, subsurface maxima in chlorophyll concentration and phytoplankton biomass are often found (Huisman et al. 2006). Such deep chlorophyll maxima are seasonal features that commonly develop in temperate (Venrick 1993) and polar oceans (Holm-Hansen & Hewes 2004). Most studies attempting to link phytoplankton with deep-diving predator behaviour are based on satellite-derived surface chlorophyll data, in part, due to the logistical constraints of sampling large and inaccessible areas of the subsurface ocean. Consequently, little is known of how top predators respond to phytoplankton density below the surface of the world's oceans.

*Corresponding author: otoolem@utas.edu.au

© Inter-Research 2017 · www.int-res.com

Marine predators foraging over thousands of kilometres must locate continuously changing prey fields and respond to complex heterogeneous environments at different scales (Russell et al. 1992). To do this, they may employ a number of different foraging strategies to locate prey (Fauchald 1999). For air-breathing marine predators, this means a trade-off between prey depth and dive capabilities (deeper prey are less likely to be exploited by air-breathing predators; Boyd 1997). Because they must return repeatedly to the surface to breathe, they are regarded as central-place foragers (Orians & Pearson 1979), with the surface acting as the central place (Houston & McNamara 1985). A major assumption is that central-place foragers will make decisions so as to maximise the net rate of energy intake during a foraging bout (Charnov 1976, Foo et al. 2016). King penguins *Aptenodytes patagonicus* use the Polar Front thermocline to gain easier access to fish prey closer to the surface (Scheffer et al. 2016), while seals will target their prey as they migrate closer to the surface during twilight hours (fur seal *Arctocephalus gazella*, Goldsworthy et al. 2010; southern elephant seal *Mirounga leonina*, McIntyre et al. 2010). These examples demonstrate how subsurface conditions influence predator access to deep-sea prey, and how this has implications for the foraging success, and ultimate survival, of deep-diving predators.

Remote sensing of surface chlorophyll via satellite has provided unprecedented insight into global spatio-temporal patterns of phytoplankton distribution in the marine environment (Field et al. 1998). While satellite observations can be used to infer chlorophyll in the upper 30 m of the water column, they do not measure deeper, sub-surface conditions (Lee et al. 2015). In oligotrophic waters, where the surface mixed layer is depleted of nutrients in summer (Holm-Hansen & Hewes 2004), subsurface chlorophyll concentration can exceed surface values by 30% (Guinet et al. 2013). Here, a subtle vertical zonation is delineated by the high-light, nutrient-poor upper euphotic layer and light-deprived, nutrient-rich lower euphotic layer (Huisman et al. 2006). Ultimately, the distribution of sub-surface phytoplankton and its extent is driven by phytoplankton type and dynamic ocean mixing (Huisman et al. 2006). An important challenge in marine ecology is to measure subsurface phytoplankton distribution and density that is concurrent with the dive behaviour of marine animals.

The need for *in situ* measurements of subsurface phytoplankton biomass has prompted researchers to explore ways to measure phytoplankton distribution that is concurrent with animal behaviour below the ocean's surface. Fluorometers attached to southern elephant seals have proven successful for estimating chlorophyll at depth (Guinet et al. 2013), but limited memory capacity and short battery life has hindered its application in large-scale studies. Alternatively, light sensors can measure bio-optical properties of the water column. This is because ambient light is attenuated by the physical properties of seawater and quantity of suspended inorganic and organic particles (Morel & Maritorena 2001). In Case I waters (dominated by phytoplankton, usually very low sedimental load), phytoplankton are the main source of suspended particles within the euphotic zone (Morel & Prieur 1977, Morel & Maritorena 2001). Light attenuation can infer phytoplankton density if we assume that physical properties are constant (Bricaud et al. 1998; and, that coloured dissolved organic matter and detritus degradation products covary with phytoplankton (Bricaud et al. 1981). Light data collected by marine animals can be used to calculate an index for phytoplankton density (Teo et al. 2009, Guinet et al. 2013) and reveal seasonal trends typical of Southern Ocean productivity (Jaud et al. 2012, O'Toole et al. 2014).

Southern elephant seals are important Southern Ocean predators that spend most of their life cycle at sea (McConnell et al. 1992). These air-breathing, deep-divers continuously dive to an average depth of 500 m (Campagna et al. 1999, McIntyre et al. 2010) where they feed predominately on mesopelagic prey (Cherel et al. 2008). Temperature and salinity sensors deployed on this species reveal their interaction with frontal and eddy features, which are thought to facilitate access to prey (Bailleul et al. 2010, Dragon et al. 2010). However, these studies lack biological information that may influence predator–prey interactions. Despite attempts to correlate satellite-derived chlorophyll with marine predator behaviour (e.g. sperm whale *Physeter macrocephalus*, Jaquet & Whitehead 1996; fur seals, Guinet et al. 2001), results remain inconclusive. Two major limitations to using satellite-derived chlorophyll data are (1) coarse, patchy resolution relative to animal behaviour; and (2) lack of subsurface information where deep-diving predators spend most of their time feeding. Recent studies have shown that elephant seal dive depth is inversely related to *in situ* light intensity, which is largely controlled by phytoplankton densities (Jaud et al. 2012, Guinet et al. 2014). This work suggested that phytoplankton may have either direct (e.g. aggregating prey) or indirect effects (e.g. shading) that facilitate seal access to prey at depth.

The oligotrophic conditions of the Southern Ocean are interspersed by regions of elevated phytoplankton biomass, including a large plume that extends for 1500 km downstream of the Kerguelen Islands (49° 15′ S, 69° 10′ E) in the Indian sector of the Southern Ocean (Blain et al. 2013). The dynamics of the Kerguelen phytoplankton plume is largely controlled by the horizontal advection of iron-rich waters from the Kerguelen Plateau and mixed-layer macronutrient inventory (Blain et al. 2007, Boyd et al. 2007, d'Ovidio et al. 2010). Phytoplankton distribution supports the proliferation of zooplankton and fish larvae (Henson et al. 2009) that ultimately influence the behaviour of top predators and their mid-trophic prey species (fish and squid). However, to date, the link between phytoplankton distribution and top predator behaviour remains poorly understood, particularly below the surface.

Following the breeding season, most female elephant seals spend 2–3 mo (October–December/early January) feeding in the vicinity of the Kerguelen phytoplankton plume (Dragon et al. 2012). We used 5 yr of animal-borne multi-sensor data to investigate how these seals and their prey respond to subsurface phytoplankton density in this large recurrent plume. First, we used light data collected by the seals to identify distinct patches of elevated phytoplankton density at the meso-scale (tens to hundreds of kilometres). We aimed to show how the horizontal structure of these patches differs in the upper euphotic layer (top 75 m of the ocean) and lower euphotic layer (75–150 m deep). Second, we used depth and accelerometer sensors to estimate subsurface prey encounter events for each seal. These data showed how diving seals responded to the structure of the Kerguelen phytoplankton plume in its upper and lower euphotic layers. Our aim was to test if phytoplankton patch density was inversely related to dive depth, and if this relationship was stronger in the upper or lower euphotic layer. The same analysis was also performed at the small scale (intra-dive) to test if seals had an immediate response to this phenomenon.

MATERIALS AND METHODS

Deployment and tag specifications

Fieldwork and data collection were approved by the Institut Polaire Francais Paul Emile Victor (IPEV) and Terres Australes et Antarctiques Francaises Animal Ethics Committee. Thirty-eight female elephant seals were equipped with either a GPS logger (n = 23) or an Argos transmitter (n = 15) (SPLASH10-Fast-Loc GPS/Argos, Wildlife Computers), in addition to a time-depth and accelerometer data logger (MK10-X or TDR10-Daily Diary, Wildlife Computers). Devices were attached to the head, except for TDR10-Daily Diary tags that were attached to the dorsal midline between the scapulae. For more details on tag deployments, see Section 1 of the Supplement at www.int-res.com/articles/suppl/m581p215_supp.pdf.

GPS locations were sampled every 20 min to maximise the chance of locations coinciding with each surface interval (see Guinet et al. 2014). The frequency of Argos locations depended on the number of available uplinks (generally between 4 and 14 locations d^{-1}). Time-depth recorders (MK10, SPLASH10 TDR and TDR10-Daily Diary) recorded time, depth (0–1500 m, ±1 m) and light levels (5×10^{-2} to 5×10^{-12} W cm^{-2} in blue wavelength) every 1 s. Acceleration was recorded in 3 axes at 16 Hz. For more details on depth, light and accelerometer specifications, see Section 1 of the Supplement.

Track estimates

GPS location estimates were up to 5 times more frequent than Argos, and location error seldom exceeded a few tens of kilometres (Lopez et al. 2014). Argos measurements were associated with varying classes of error and were processed using a multiple-model Kalman filter (Lopez et al. 2014). Kalman-smoothed Argos locations were provided at the time of each original Argos location. Tracks were interpolated from either GPS or Argos locations, and each dive was given a geographical coordinate based on its position in time along the track. We used data from 23 female southern elephant seal deployments between 2010 and 2013 that migrated eastward from the Kerguelen Islands. The seals foraged within a large phytoplankton plume (70–110° E and 60–40° S) that reoccurs annually during early austral spring/summer (October–February; Moore & Abbott 2000) (Fig. 1).

Dive profiles

All dive records were corrected for drift in the pressure sensor using a customised zero-offset correction routine (see Heerah et al. 2014). We then identified individual dives, defined here as commencing from the first subsurface record until the

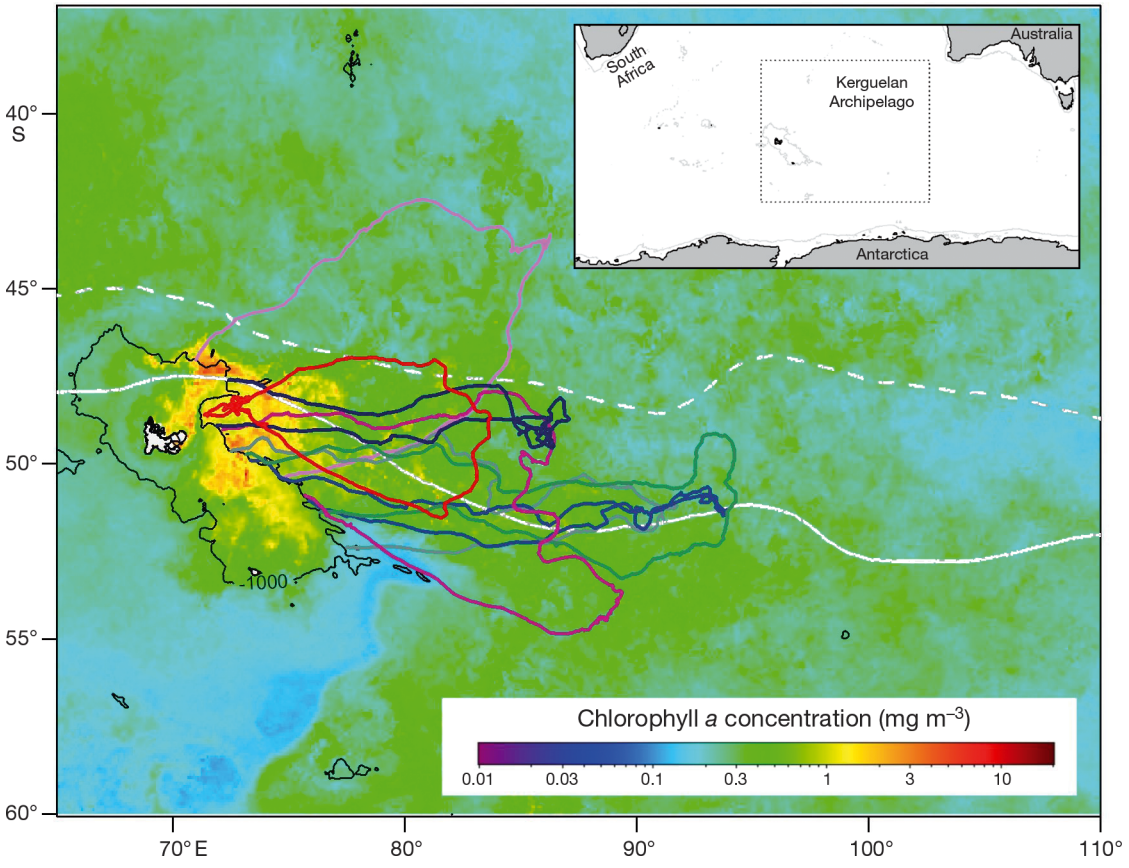

Fig. 1. Tracks of post-breeding female southern elephant seals *Mirounga leonina* (n = 15) superimposed over the Kerguelen phytoplankton plume (chlorophyll concentration composite Nov/Dec 2010–2013). The Kerguelen shelf break is denoted by the 1000 m isobath (thin black solid line); and ocean fronts include the sub-Antarctic Front (SAF, dashed) and Polar Front (PF, solid line). Chlorophyll concentration data were from the Aqua MODIS Chlorophyll Concentration (OCx Algorithm) Ocean Color Data, NASA, http://oceancolor.gsfc.nasa.gov/cgi/l3

last surface record of the subsequent post-dive surface interval. Each dive was divided into 3 phases: descent, bottom and ascent. The descent phase was from the surface (0 m) to 80% of the maximum dive depth; the bottom phase was below the 80% maximum dive depth threshold; and the ascent phase was from the end of the bottom phase to the surface. Dive depth was defined as the mean depth of the bottom phase.

Female southern elephant seals mainly feed in oceanic waters (but also over the Kerguelen Plateau and Antarctic continental shelves). We focused on pelagic dives and excluded dives performed on the Kerguelen and Crozet Plateaus (i.e. <1000 m bathymetry depth) where the food web is different. We used bathymetric data from National Geophysical Data Centre ETOPO2 Global 2 Elevations (www.ngdc.noaa.gov/mgg/global/etopo2.html), which provided sufficient resolution for our analyses.

Prey encounter events (PEEs)

Data from the accelerometers were processed according to Viviant et al. (2010) and Gallon et al. (2013) using custom-written MATLAB code (available on request). Individual putative feeding events were detected from accelerometer data using procedures outlined by Guinet et al. (2014). The steps in this procedure include (1) a high-pass filter of 0.33 critical frequency of the 3-axis accelerometer time series to remove noise due to swimming movement and (2) identifying significant accelerations along each axis time series (summed to 1 s resolution). For more detail on PEE detection see Section 2 of the Supplement. PEEs were calculated as a rate (min^{-1}) in the dive bottom phase, where elephant seals are thought to perform most of their foraging activity (Heerah et al. 2014). Detecting PEEs using accelerometer data does not necessarily reflect a true feeding

event (Watanabe & Takahashi 2013), and for this study, is instead considered as a relative index of prey encounters during the bottom phase of the dive.

Phytoplankton density estimates derived from light: mesoscale and small scale

Light levels (LLs) collected from animal-borne sensors can be used as a proxy for relative phytoplankton density (for details see O'Toole et al. 2014). We minimised error by using LLs recorded in the top 200 m of the water column when sun angle is >10° (day), because light sensor sensitivity is reduced below 200 m deep and at night (Wildlife Computers pers. comm.). Sun angle was calculated using the R software package *TripEstimation* (R Development Core Team 2016, function *astro*; Sumner & Wotherspoon 2013). Body roll of the animal can also affect light sensor records, and we only used LLs recorded in the ascent phase of each dive where incidence of body roll is low (Sala et al. 2011). LLs as a function of depth are plotted in Section 3 of the Supplement. For each dive, LLs were interpolated linearly between the non-regular series of depths at the boundary of 2 layers of the euphotic zone: the upper euphotic layer (0–75 m) and lower euphotic layer (75–150 m). LL at 0 m was taken as the mean LL recorded in the last 10 m of the dive ascent to minimise the effects of surface quenching (see Guinet et al. 2013). Phytoplankton density in the upper euphotic layer (P_{upper}) was inferred by calculating the difference between LLs at 75 m (LL_{75}) and 0 m (LL_0), divided by the difference in depth:

$$\frac{(LL_{75} - LL_0)}{(\Delta 75\ m - 0\ m)} \sim P_{upper} \quad (1)$$

Phytoplankton density in the lower euphotic layer (P_{lower}) was inferred by calculating the difference between LLs at 150 m (LL_{150}) and 75 m (LL_{75}), divided by the difference in depth:

$$\frac{(LL_{150} - LL_{75})}{(\Delta 150\ m - 75\ m)} \sim P_{lower} \quad (2)$$

To identify patches of high and low phytoplankton density, a cubic smoothing spline was fitted to the time series of P_{upper} and P_{lower} for each trip using the R software package *stats* (function smooth.spline, R Development Core Team 2016). The number of knots applied to this function was based on the total number of days spent in the oceanic zone divided by 4 d. The 4 d interval was used as this is the approximate time taken for an elephant seal to pass across mesoscale features (Cotté et al. 2015) if we assume an average diameter of 300 km and seals' daily horizontal displacement to be 75 km d^{-1} (average daily displacement of seals in this study was 62 ± 42 km d^{-1}). Values from the smoothing spline were then used to identify distinct patches of high phytoplankton density and low phytoplankton density encountered by seals along their track. For details of this procedure, see Section 4 of the Supplement.

Elephant seal response to phytoplankton estimates: mesoscale and small scale

We performed permutation analyses at the mesoscale to test the null hypothesis that PEE and seal dive depth were not different between high and low phytoplankton density patch groups (P_{upper}, P_{lower}) (Good 2005). We computed the mean for each group and calculated the difference of these means (D_{obs}). We then permuted P_{upper}+ P_{lower} observations between the 2 treatments (permutations, ε = 500), obtained all possible permutations and calculated the p-value (for R code, see Section 5 of the Supplement). This was also repeated for each individual seal.

We also examined small (inter-dive) scale seal behavioural response to P_{upper} or P_{lower} (predictor) and a phytoplankton patch density interaction term ($P_{density}$) using linear mixed-effect models from the R software package *nlme* (R Development Core Team 2016, function lme; Pinheiro et al. 2015):

$$PEE \sim P_{upper} \times P_{density} \quad (3)$$

$$\text{Dive depth} \sim P_{upper} \times P_{density} \quad (4)$$

$$PEE \sim P_{lower} \times P_{density} \quad (5)$$

$$\text{Dive depth} \sim P_{lower} \times P_{density} \quad (6)$$

Individual was included as a random effect. Details of the statistical method are outlined by Zuur et al. (2011). Variables were transformed, where necessary, prior to analyses to correct for non-Gaussian distributions. We could not use zero-inflated Poisson or negative binomial models because PEEs were not count data. Consequently, dives where PEE = 0 were removed (upper euphotic layer, n = 488 or 13.2%; lower euphotic layer, n = 482 or 17.1%).

RESULTS

Of the 23 female southern elephant seals in this study, only 15 recorded PEEs for more than 20 d

(Table 1). All other tracks were excluded from subsequent analyses due to tag failure or memory issues. Of the 15 seals, most (n = 12) travelled eastward within the Polar Frontal Zone and along the southern edge of the Polar Front, while 3 other seals travelled north-east from Kerguelen to the Subantarctic Zone; all were within the recurrent phytoplankton plume east of the Kerguelen Plateau (Fig. 1). One seal (ID: 2010-18) recorded time, depth, light and accelerometer data for the entire trip; 10 recorded time, depth and light data for the entire trip and accelerometer data for part of the trip; and 4 recorded time, depth, light and accelerometer data for only part of the trip (Table 1; see mapped data availability in Section 6 of the Supplement). Between 2010 and 2013, seals entered the pelagic zone (east of the Kerguelen Plateau) in late October or early November and returned to the plateau in late November or late December (Table 1). In total, tag deployments recorded 31 884 dive profiles during daylight hours (sun 10° above horizon), of which <2% were removed (1.02% shelf dives, 0.02% drift dives and <0.01% dives corresponding with negative light attenuation values). Of the remaining dive profiles, 17 189 contained concurrent accelerometer data. The number of dives associated with PEEs (i.e. PEE rate > 0) was 47.0% (N = 8079) of dives with accelerometer records. For most dives (97%), the bottom phase and PEEs were recorded well below the euphotic zone (200–1100 m deep).

Table 1. Female southern elephant seal *Mirounga leonina* identification, time spent in the pelagic zone (beyond 1000 m shelf break) and data records. (++) Time, depth, light and accelerometer data recorded for the entire trip; (+–) time, depth, light recorded over the entire trip, accelerometer recorded for part of the trip; (––) time, depth, light and accelerometry data recorded for part of the trip

Seal ID	Time spent in pelagic zone			Data records
	Start	End	Days	
2010-18	30 Oct 2010	21 Dec 2010	52	++
2011-21	31 Oct 2011	21 Dec 2011	51	+–
2011-26	02 Nov 2011	26 Dec 2011	54	+–
2011-28	02 Nov 2011	24 Dec 2011	52	+–
2012-1	29 Oct 2012	20 Nov 2012	23	+–
2012-11	04 Nov 2012	26 Nov 2012	22	––
2012-14	03 Nov 2012	29 Nov 2012	26	––
2012-16	04 Nov 2012	26 Nov 2012	22	––
2012-17	04 Nov 2012	27 Nov 2012	23	––
2012-3	31 Oct 2012	22 Nov 2012	22	+–
2012-4	30 Oct 2012	20 Nov 2012	21	––
2012-6	01 Nov 2012	22 Nov 2012	21	+–
2013-1	30 Oct 2013	23 Nov 2013	24	+–
2013-3	01 Nov 2013	21 Nov 2013	21	+–
2013-7	31 Oct 2013	25 Nov 2013	26	+–

Elephant seal response to phytoplankton estimates: mesoscale

Mesoscale patches of high and low phytoplankton density (hereafter high- and low-density patches, respectively), as derived by light data, were encountered by each seal, but the timing and location of these patches differed between the upper and lower euphotic layers (Fig. 2). We found significant differences in both euphotic layers between (1) PEEs below high- and low-density patches (Fig. 3a,b) and (2) dive depth below high- and low-density patches (Fig. 3c,d).

First, seals recorded significantly more PEEs and shallower dives below high-density patches compared to low-density patches in both layers of the euphotic zone (Fig. 3). For the upper euphotic layer, the average PEE was 0.70 min^{-1} below high-density patches and 0.66 min^{-1} below low-density patches (ΔPEE = 0.04, p = 0.004; Fig. 3a). For the lower euphotic layer, the average PEE was 0.67 min^{-1} below high-density patches and 0.57 min^{-1} below low-density patches (Fig. 3b). However, PEE differences below high- and low-density patches in the lower euphotic layer were marginally stronger (ΔPEE = 0.1, p < 0.0001; Fig. 3b) than differences in the upper euphotic layer (Fig. 3a). The highest average PEE was below high-density patches in the upper euphotic layer (0.70 PEE min^{-1}; Fig. 3a), and the lowest average PEE was below low-density patches in the lower euphotic layer (0.57 PEE min^{-1}; Fig. 3b).

Second, the average dive depth below upper euphotic layer patches was 519 m below high-density patches and 567 m below low-density patches (Δdive depth = 48 m, p < 0.0001; Fig. 3c). For the lower euphotic layer, we showed the same effect, but stronger: average dive depth was 483 m below high-density patches and 571 m below low-density patches (Δdive depth = 88 m, p < 0.0001; Fig. 3d). The average dive depth was shallowest below high-density patches in the lower euphotic layer (483 m) and deepest below low-density patches in the same layer (571 m; Fig. 3d).

At the individual level (N = 15), we found that PEEs and dive depth varied in response to high- and low-density patches within the euphotic zone (Fig. 4, Table 2). For upper euphotic layer conditions, 6 seals recorded significantly higher PEEs below high-density patches and 3 recorded significantly higher PEEs below low-density patches. Most seals (N = 9) dived significantly deeper below low-density patches, and only 2 dived significantly deeper below dense patches. For lower euphotic layer conditions, no seals recorded significantly higher PEEs below low-

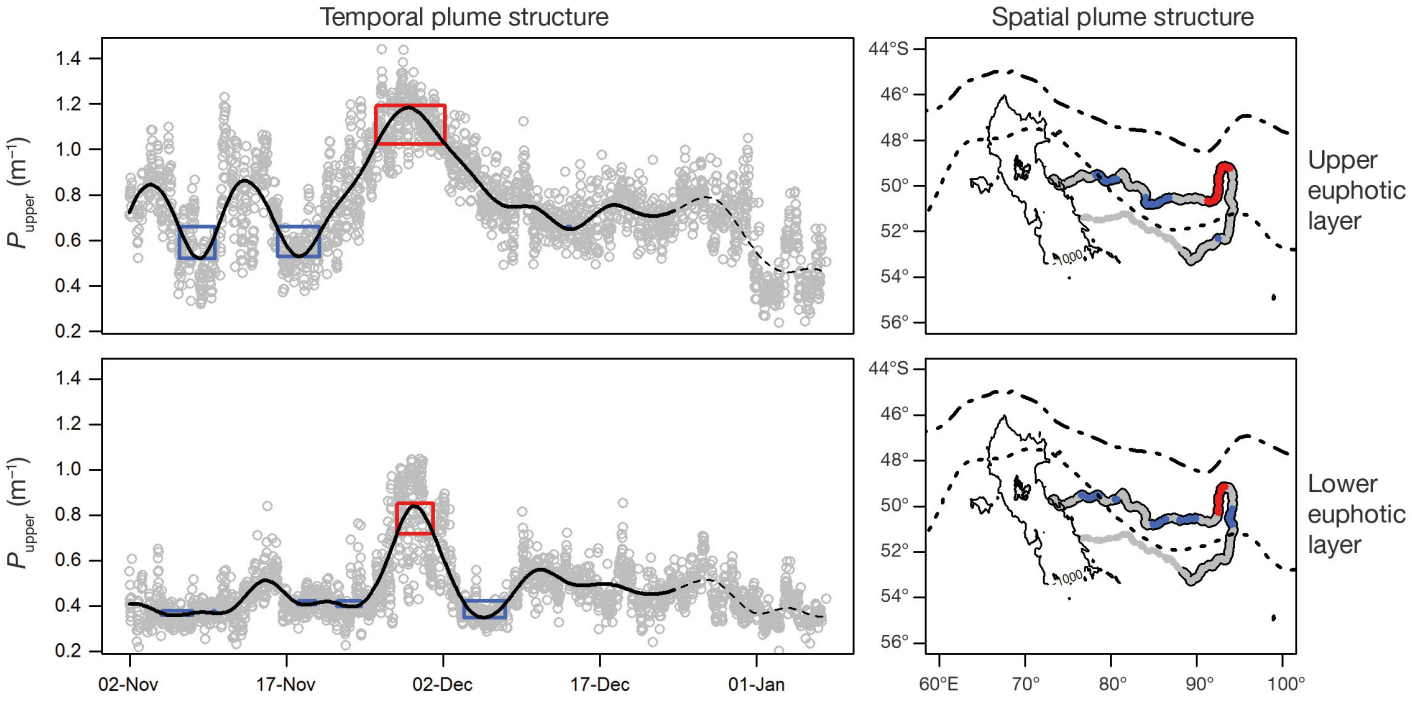

Fig. 2. Phytoplankton distribution encountered by female southern elephant seals *Mirounga leonina* at the mesoscale. The temporal pattern (left column) of phytoplankton is represented by a smoothed black trend line (line is dashed where accelerometer data were not recorded). Grey circles are the original intra-dive phytoplankton density estimates, and coloured boxes represent mesoscale patches of high- and low-density phytoplankton (red and blue, respectively). P_{upper} (P_{lower}): phytoplankton density in the upper (lower) euphotic layer. The spatial pattern (right column) of phytoplankton corresponds with its temporal pattern. The Kerguelen shelf break is denoted by the 1000 m isobath (solid line), and ocean fronts include the sub-Antarctic Front (SAF, dot-dashed) and Polar Front (PF, dotted). Data were recorded by seal no. 2011-28. For data recorded by all other seals, see Section 6 of the Supplement

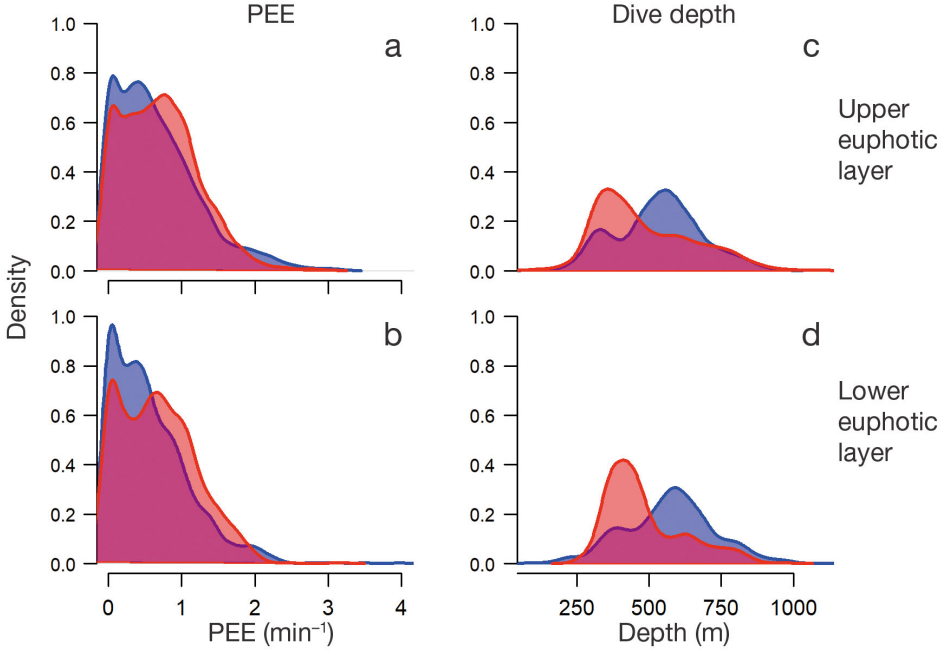

Fig. 3. Female southern elephant seal *Mirounga leonina* behavioural responses below mesoscale patches of phytoplankton: (a,b) prey encounter event (PEE) response; (c, d) dive depth response. Behavioural responses were compared between high- and low-density patches of phytoplankton (red and blue, respectively). Behavioural responses were recorded below patches of phytoplankton in the upper and euphotic layers. Data are from all seals (n = 15). For individual seal plots, see Section 7 of the Supplement

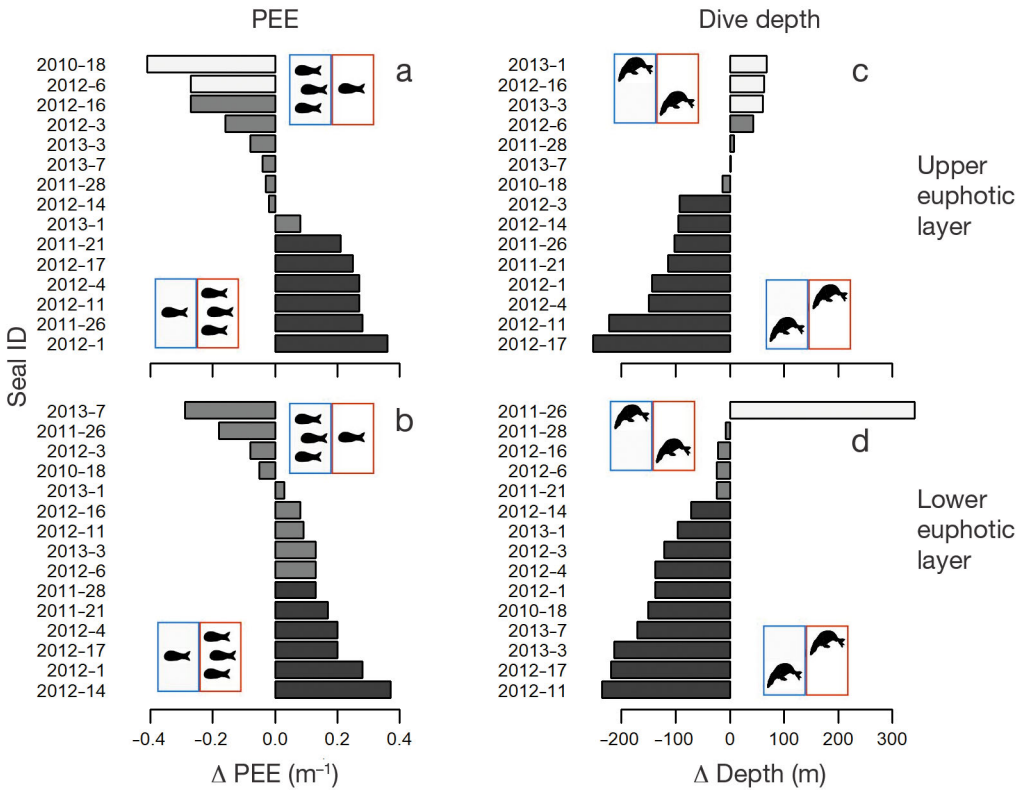

Fig. 4. Red, blue boxes: relative behavioural difference between high- and low-density plankton patches, respectively, for each female southern elephant seal *Mirounga leonina*: (a,b) mean difference in prey encounter events (Δ PEE) and (c,d) dive depth (Δ Depth). Analyses were performed in the upper euphotic layer (a,c) and lower euphotic layer (b,d). Shaded bars — dark grey: significant ($p < 0.05$) negative differences; light grey: significant positive differences; mid grey: non-significant differences. Graphics in boxes represent relative differences: multiple fish symbols (high PEE) versus single fish symbol (low PEE); upper seal symbol (shallow dives) versus lower seal symbol (deeper dives)

density patches, and only 6 seals recorded significantly higher PEEs below high-density patches. No seals dived significantly deeper below high-density patches, but as many as 11 seals dived significantly deeper below low-density patches. (Individual plots are available in Section 7 of the Supplement).

Elephant seal response to phytoplankton estimates: small scale (intra-dive)

We found that small-scale phytoplankton density within high- and low-density patches was positively related to (1) higher PEEs and (2) shallower dives (Fig. 5a,c,d). Our most parsimonious model in Fig. 5a, where PEE is the response, also included mesoscale patch density as an interaction term (high- vs. low-density patches; see Table 3). This interaction term showed that the PEE response to small-scale phytoplankton density in the upper euphotic layer was stronger below high-density mesoscale patches compared with low-density mesoscale patches (Fig. 5a). We found no significant PEE response to phytoplankton conditions in the lower euphotic layer (Fig. 5b). We did, however, find that dive depth response to small-scale phytoplankton density was significant in both layers of the euphotic zone (Fig. 5c,d), although the slope coefficient was higher under conditions in the upper euphotic layer (Table 3).

DISCUSSION

Ecological connections between surface waters and the deep ocean remain poorly studied despite the high biomass of fishes and squids residing at depths beyond the euphotic zone. We found that deep-diving southern elephant seals (SES) foraging in open waters of the Kerguelen phytoplankton plume responded to different scales and vertical distribution of phytoplankton.

Studies have shown no clear relationship between predator foraging behaviour and phytoplankton (Jaquet & Whitehead 1996, Bradshaw et al. 2004), although Guinet et al. (2001) found contrasting results showing that dive activity of fur seals was negatively

Table 2. Relative differences of female southern elephant seal *Mirounga leonina* behavioural responses (prey encounter events [PEEs] and dive depth) below mesoscale patches of high- and low-density phytoplankton ($Patch_{high}$ and $Patch_{low}$, respectively) in the upper and lower euphotic layer (see Fig. 4). (Δ) Relative differences; **bold:** significant response between $Patch_{low}$ and $Patch_{high}$

Seal ID	PEEs (min^{-1})				Dive depth (m)			
	$Patch_{low}$	$Patch_{high}$	Δ	p	$Patch_{low}$	$Patch_{high}$	Δ	p
Upper								
2012-1	**0.73**	**1.09**	**0.36**	**<0.0001**	**586**	**442**	**−144**	**<0.0001**
2011-26	**0.89**	**1.17**	**0.28**	**<0.0001**	**655**	**553**	**−102**	**0.002**
2012-11	**0.59**	**0.86**	**0.27**	**<0.0001**	**602**	**379**	**−223**	**<0.0001**
2012-4	**0.7**	**0.98**	**0.27**	**<0.0001**	**617**	**466**	**−150**	**<0.0001**
2012-17	**0.58**	**0.83**	**0.25**	**<0.0001**	**659**	**408**	**−252**	**<0.0001**
2011-21	**0.65**	**0.85**	**0.21**	**0.002**	**662**	**549**	**−114**	**<0.0001**
2013-1	0.76	0.84	0.08	0.46	**569**	**636**	**68**	**<0.0001**
2012-14	0.87	0.84	−0.02	0.816	**496**	**401**	**−95**	**<0.0001**
2011-28	0.91	0.88	−0.03	0.384	387	394	7	0.28
2013-7	0.51	0.47	−0.04	0.438	634	635	2	0.91
2013-3	0.95	0.87	−0.08	0.526	584	646	61	0.012
2012-3	0.71	0.56	−0.16	0.098	**536**	**444**	**−93**	**<0.0001**
2012-16	0.78	0.51	−0.27	0.002	580	643	63	<0.0001
2012-6	0.95	0.68	−0.27	0.036	578	622	43	0.09
2010-18	0.88	0.48	−0.41	<0.0001	691	677	−14	0.442
Lower								
2012-14	**0.72**	**1.09**	**0.37**	**<0.0001**	**515**	**443**	**−72**	**<0.0001**
2012-1	**0.8**	**1.08**	**0.28**	**0.004**	**555**	**418**	**−138**	**<0.0001**
2012-17	**0.59**	**0.79**	**0.2**	**0.046**	**650**	**430**	**−220**	**<0.0001**
2012-4	**0.82**	**1.02**	**0.2**	**<0.0001**	**600**	**462**	**−138**	**<0.0001**
2011-21	**0.61**	**0.78**	**0.17**	**0.05**	611	587	−25	0.22
2011-28	**0.79**	**0.92**	**0.13**	**0.006**	398	390	−8	0.338
2012-6	0.62	0.75	0.13	0.214	646	620	−25	0.35
2013-3	0.71	0.84	0.13	0.396	**743**	**529**	**−213**	**<0.0001**
2012-11	0.58	0.67	0.09	0.056	**619**	**382**	**−236**	**<0.0001**
2012-16	0.42	0.5	0.08	0.248	664	642	−22	0.314
2013-1	0.53	0.56	0.03	0.7	**670**	**574**	**−96**	**<0.0001**
2010-18	0.55	0.5	−0.05	0.28	**774**	**623**	**−151**	**<0.0001**
2012-3	0.64	0.56	−0.08	0.288	**565**	**444**	**−121**	**<0.0001**
2011-26	1.09	0.91	−0.18	0.376	**351**	**692**	**341**	**<0.0001**
2013-7	0.47	0.18	−0.29	0.08	**665**	**495**	**−171**	**<0.0001**

related to chlorophyll *a* concentration at small spatial scale (<0.3° grid cells) and positively related at larger scales (2° grid cells). It is likely that these studies were limited by 2 fundamental problems: (1) the spatio-temporal mismatch between the satellite-derived chlorophyll data (10s of kilometres and days) and animal foraging behaviour (100s of metres and minutes); and (2) satellite data only provide information at the near-surface. Although our *in situ* light-based estimates of phytoplankton density do not represent absolute values, the effectiveness of light as a proxy for plankton density has been demonstrated (Teo et al. 2009, O'Toole et al. 2014). Light used to estimate phytoplankton density attempts to address the 2 fundamental problems cited above.

The Kerguelen Plateau sustains the most productive waters in the Antarctic Circumpolar Circulation (Moore & Abbott 2000, Chever et al. 2010) and enriches waters thousands of kilometres downstream via lateral advection (Blain et al. 2001, Sokolov & Rintoul 2007, Mongin et al. 2009) to form what we term the 'Kerguelen phytoplankton plume'. All elephant seals in our study foraged within this plume during their post-breeding foraging trips. Our *in situ* proxy for phytoplankton density revealed seals travelling through alternating patches of high- and low-density phytoplankton. The timing and location of these patches varied between the upper and lower layers of the euphotic zone. Planktonic features of these patches in the euphotic zone are likely driven by mesoscale eddy processes that can be observed in this region using multi-satellite maps (d'Ovidio et al. 2010). The encounter between seal 2012-28 and a known eddy feature (Della Penna et al. 2015), which often facilitates the accumulation of phytoplankton (d'Ovidio et al. 2013), was identified by our analysis as a high-density patch of phytoplankton, helping to confirm our approach.

Although elephant seals forage continuously while migrating (Thums et al. 2011), optimal foraging theory predicts that animals will make decisions (at various scales) to maximise the net rate of energy intake (Charnov 1976). At the basin scale, Southern Ocean predators will use major fronts and shelf edges (e.g. Charrassin et al. 2002, Lea et al. 2002a). At finer scales, predators will respond to the accumulative and retentive effects of ocean physics on biological communities (e.g. Polovina et al. 2006, Cherel et al. 2007, Bailleul et al. 2010, Cotté et al. 2015). Diving animals require additional feeding strategies to compensate for physiological diving constraints when searching for deep-dwelling prey like myctophids. King penguins use the Polar Front thermocline to target myctophids that aggregate at relatively shallow depths (Scheffer et al. 2016). Diving predator species, including elephant seals, will follow the diel vertical migration patterns of their

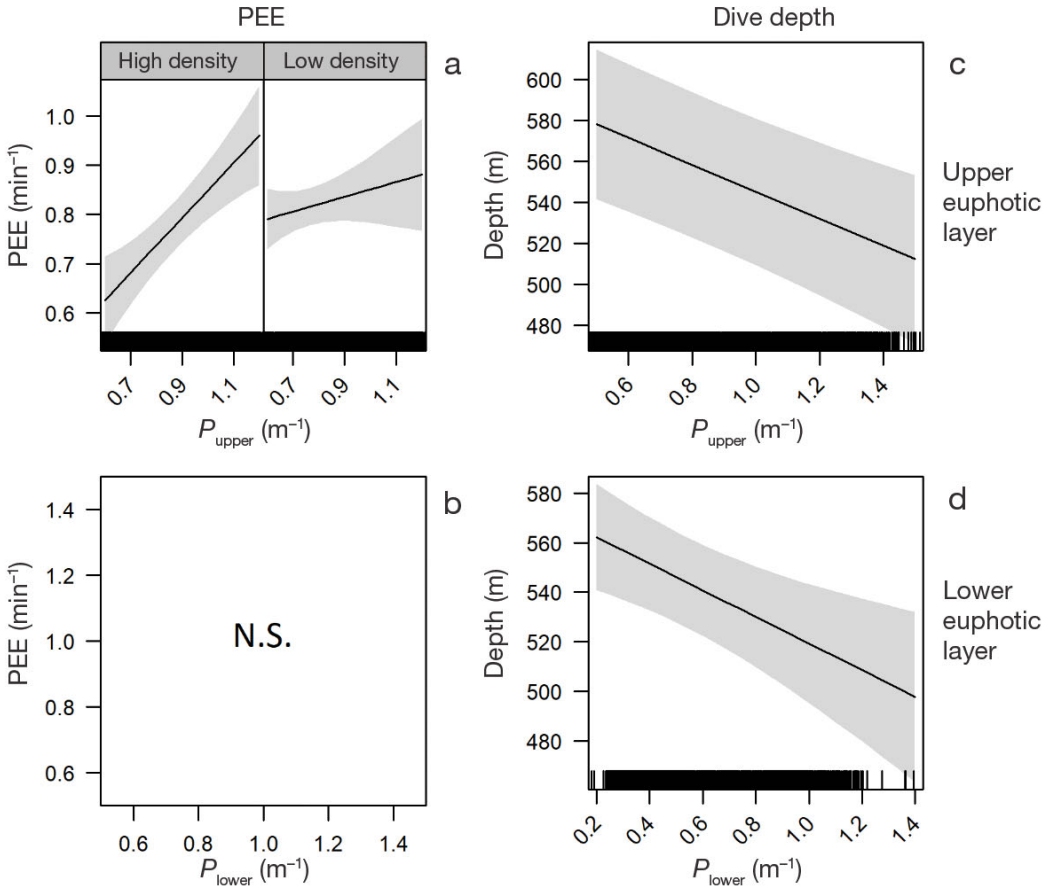

Fig. 5. Female southern elephant seal *Mirounga leonina* inter-dive behavioural response below layers of phytoplankton: (a,b) prey encounter event (PEE) response and (c,d) dive depth response. Behavioural response is recorded below small-scale phytoplankton distribution in the upper (P_{upper}) and lower (P_{lower}) euphotic layers. Analyses were performed using linear mixed effect models and include an interaction term effect between mesoscale patches of high- and low-density phytoplankton (panel a). Shaded areas: confidence intervals. Includes data from all seals (n = 15). PEE response to P_{lower} was non-significant (N.S.). Rugplots (original data points) in (a,c,d) show spread of the data

Table 3. Linear mixed effect model analyses of female southern elephant seal *Mirounga leonina* behavioural responses to phytoplankton between dives (small scale). Behavioural responses include prey encounter events (PEEs) and dive depth, and were examined below the upper euphotic layer (P_{upper}) and lower euphotic layer (P_{lower}) in separate models. $P_{density}$ is a factor with 2 levels: high- and low-density phytoplankton patches. An interaction term effect (P_{upper}: $P_{density}$) was included if retained after our model selection procedure (see 'Materials and methods')

	Coefficient	SE	df	*t*	p
PEE ~ P_{upper} + $P_{Density}$ + P_{upper}: $P_{density}$					
Intercept	0.29	0.12	3200	2.34	0.0194
P_{upper}	0.56	0.14	3200	4.02	0.0001
$P_{density}$ (Low)	0.41	0.11	3200	3.71	0.0002
P_{upper}: $P_{density}$ (Low)	−0.41	0.12	3200	−3.37	0.0008
Depth ~ P_{upper} + $P_{density}$					
Intercept	587.74	24.16	3201	24.33	<0.0001
P_{upper}	−65.81	15.31	3201	−4.30	<0.0001
$P_{density}$ (Low)	44.79	11.10	3201	4.04	0.0001
Depth ~ P_{lower} + $P_{density}$					
(Intercept)	533.55	17.68	2317	30.17	<0.0001
P_{lower}	−53.57	17.12	2317	−3.13	0.0018
$P_{density}$ (Low)	62.41	15.71	2317	3.97	0.0001

prey throughout the day (McIntyre et al. 2010). Elephant seal dive depth also varies during daylight hours in response to light levels at depth, which are thought to be largely influenced by phytoplankton concentrations (Jaud et al. 2012). A similar trend with SES was apparent in the study by Guinet et al. (2014), although no distinction was made between the upper and lower euphotic layer in either study, nor a comparison between mesoscale patches of high- and low-density phytoplankton.

At the mesoscale, denser patches of phytoplankton were linked to higher PEEs and shallower dive depth recorded by SES below the euphotic zone. This link was

stronger below patches of phytoplankton in the lower euphotic layer. The heterogeneous distribution of phytoplankton is likely to aggregate prey biomass via mesoscale processes including convergence regions and tracer fronts (d'Ovidio et al. 2015), as well as localised retention (d'Ovidio et al. 2013). High prey density would lead to high predator densities, and forms a direct link between elephant seals and their prey (e.g. myctophids, Cherel et al. 2008).

At the small scale, phytoplankton density fluctuations between dives may act as an indirect link between SES and their prey. We propose that the phytoplankton density gradient is large enough to influence seal vertical access to their prey via its shading effect (an indirect link). Our results suggest that this influence is more likely from phytoplankton density in the upper euphotic layer. Light plays a crucial role in the vertical distribution of a broad range of mesopelagic organisms, including myctophids (Catul et al. 2011), and is likely a predator-avoidance mechanism (Bollens et al. 1992, Liu et al. 2003). Consequently, myctophids are expected to be found closer to the surface when ambient light levels are comparatively low. If shading is the main mechanism driving SES access to prey at the small scale, then Fig. 5 suggests that its greatest impact should be observed below high-density patches of phytoplankton in the upper euphotic layer. The importance of shading could be inflated further around noon (local time) when light intensity is expected to peak (see Section 8 of the Supplement).

In this study, there was also considerable individual variation. Most SES performed shallower dives below high-density patches of phytoplankton, but fewer SES recorded higher PEEs below the same patch. Grazing zooplankton may dominate a system later in the season when phytoplankton stocks become depleted (Jouandet et al. 2011). This can lead to high zooplankton, and consequently, high fish stocks, below patches where phytoplankton density is low. Advected water parcels associated with high primary production at the beginning of the season may drift away from the location of a bloom event (d'Ovidio et al. 2015). Zooplankton that drift passively with these productive water parcels, and mid-trophic fish that actively follow zooplankton, will aggregate in these patches long after conditions were favourable for phytoplankton growth (Loots et al. 2007). Cotté et al. (2015) were able to use semi-Lagrangian diagnostics to track water parcels from their origin in a phytoplankton plume on the Kerguelen Plateau. These productive water parcels were followed by the SES as they drifted eastward despite the lack of phytoplankton stocks later on in the season, presumably because these stocks were depleted by grazers that proliferate soon after the bloom season (Robins et al. 1995).

In a small number of individuals, we found that phytoplankton density had no effect on dive depth. We suspect that SES adjust their foraging strategy in response to other environmental factors, effectively overriding a strategy that allows them to exploit the shading effect of phytoplankton. For example, seal 2012-28 encountered the largest change in phytoplankton density in our study, and yet, her dive depth did not vary with mesoscale phytoplankton density. We know from Della Penna et al. (2015) that this same seal increased its vertical displacement in order to drift passively with an aggregate of prey below the high-density patch of phytoplankton identified in our study. This may help explain why some SES were more likely to dive deeper in patches of high-density phytoplankton.

All of the SES that did record shallower dives below high-density patches of phytoplankton (N = 11) were >70 m less than dives below low-density patches. In some cases, the difference could be >200 m less. This difference is important for deep-diving species that need to maximise net rate of energy intake for improved survival. The direct and indirect effects of phytoplankton discussed here may therefore be relevant to other deep-diving predator species, particularly species that are constrained more than SES by their dive physiology (e.g. fur seals, Lea et al. 2002b; king penguins, Scheffer et al. 2016). Finally, the foraging strategies of top predators are expected to be implicated by the future warming of the world's oceans if prey dive deeper to avoid warmer surface layers (e.g. myctophids, Péron et al. 2012).

Acknowledgements. The seal tracking data were collected by the Integrated Marine Observing System (IMOS). IMOS is a national collaborative research infrastructure, supported by the Australian Government, that is operated by a consortium of institutions as an unincorporated joint venture, with the University of Tasmania as Lead Agent. All animals in this study were treated in accordance with the guidelines of the IPEV and Polar Environment ethics committees. We thank everyone who contributed to the field work, with special thanks to N. El Skaby. Thanks also to Baptiste Picard for processing and collating track datasets.

LITERATURE CITED

Bailleul F, Cotté C, Guinet C (2010) Mesoscale eddies as foraging area of a deep-diving predator, the southern elephant seal. Mar Ecol Prog Ser 408:251–264

Blain S, Tréguer P, Belviso S, Bucciarelli E and others (2001) A biogeochemical study of the island mass effect in the con-

text of the iron hypothesis: Kerguelen Islands, Southern Ocean. Deep Sea Res Part I Oceanogr Res Pap 48:163–187
Blain S, Quéguiner B, Armand L, Belviso S and others (2007) Effect of natural iron fertilization on carbon sequestration in the Southern Ocean. Nature 446:1070–1074
Blain S, Renaut S, Xing X, Claustre H, Guinet C (2013) Instrumented elephant seals reveal the seasonality in chlorophyll and light-mixing regime in the iron-fertilized Southern Ocean. Geophys Res Lett 40:6368–6372
Bollens SM, Frost BW, Thoreson DS, Watts SJ (1992) Diel vertical migration in zooplankton: field evidence in support of the predator avoidance hypothesis. Hydrobiologia 234:33–39
Boyd IL (1997) The behavioural and physiological ecology of diving. Trends Ecol Evol 12:213–217
Boyd PW, Jickells T, Law CS, Blain S and others (2007) Mesoscale iron enrichment experiments 1993-2005: synthesis and future directions. Science 315:612–617
Bradshaw CJA, Higgins J, Michael KJ, Wotherspoon SJ, Hindell MA (2004) At-sea distribution of female southern elephant seals relative to variation in ocean surface properties. ICES J Mar Sci 61:1014–1027
Bricaud A, Morel A, Prieur L (1981) Absorption by dissolved organic matter of the sea (yellow substance) in the UV and visible domains. Limnol Oceanogr 26:43–53
Bricaud A, Morel A, Babin M, Allali K, Claustre H (1998) Variations of light absorption by suspended particles with chlorophyll *a* concentration in oceanic (case 1) waters: analysis and implications for bio-optical models. J Geophys Res Oceans 103:31033–31044
Campagna C, Fedak M, McConnell BJ (1999) Post-breeding distribution and diving behavior of adult male southern elephant seals from Patagonia. J Mammal 80:1341–1352
Catul V, Gauns M, Karuppasamy PK (2011) A review on mesopelagic fishes belonging to family Myctophidae. Rev Fish Biol Fish 21:339–354
Charnov EL (1976) Optimal foraging, the marginal value theorem. Theor Popul Biol 9:129–136
Charrassin JB, Park YH, Le Maho Y, Bost CA (2002) Penguins as oceanographers unravel hidden mechanisms of marine productivity. Ecol Lett 5:317–319
Cherel Y, Hobson KA, Guinet C, Vanpe C (2007) Stable isotopes document seasonal changes in trophic niches and winter foraging individual specialization in diving predators from the Southern Ocean. J Anim Ecol 76:826–836
Cherel Y, Ducatez S, Fontaine C, Richard P, Guinet C (2008) Stable isotopes reveal the trophic position and mesopelagic fish diet of female southern elephant seals breeding on the Kerguelen Islands. Mar Ecol Prog Ser 370: 239–247
Chever F, Sarthou G, Bucciarelli E, Blain S, Bowie AR (2010) An iron budget during the natural iron fertilisation experiment KEOPS (Kerguelen Islands, Southern Ocean). Biogeosciences 7:455–468
Cotté C, d'Ovidio F, Dragon AC, Guinet C, Lévy M (2015) Flexible preference of southern elephant seals for distinct mesoscale features within the Antarctic Circumpolar Current. Prog Oceanogr 131:46–58
d'Ovidio F, De Monte S, Alvain S, Dandonneau Y, Levy M (2010) Fluid dynamical niches of phytoplankton types. Proc Natl Acad Sci USA 107:18366–18370
d'Ovidio F, De Monte S, Della Penna A, Cotté C, Guinet C (2013) Ecological implications of eddy retention in the open ocean: a Lagrangian approach. J Phys A Math Theor 46:254023
d'Ovidio F, Della Penna A, Trull TW, Nencioli F and others (2015) The biogeochemical structuring role of horizontal stirring: Lagrangian perspectives on iron delivery downstream of the Kerguelen Plateau. Biogeosciences 12: 5567–5581
Della Penna A, De Monte S, Kestenare E, Guinet C, d'Ovidio F (2015) Quasi-planktonic behavior of foraging top marine predators. Sci Rep 5:18063
Dragon AC, Monestiez P, Bar-Hen A, Guinet C (2010) Linking foraging behaviour to physical oceanographic structures: southern elephant seals and mesoscale eddies east of Kerguelen Islands. Prog Oceanogr 87:61–71
Dragon AC, Bar-Hen A, Monestiez P, Guinet C (2012) Horizontal and vertical movements as predictors of foraging success in a marine predator. Mar Ecol Prog Ser 447: 243–257
Fauchald P (1999) Foraging in a hierarchical patch system. Am Nat 153:603–613
Field CB, Behrenfeld MJ, Randerson JT, Falkowski P (1998) Primary production of the biosphere: integrating terrestrial and oceanic components. Science 281:237–240
Foo D, Semmens JM, Arnould JPY, Dorville N and others (2016) Testing optimal foraging theory models on benthic divers. Anim Behav 112:127–138
Gallon S, Bailleul F, Charrassin JB, Guinet C, Bost CA, Handrich Y, Hindell M (2013) Identifying foraging events in deep diving southern elephant seals, *Mirounga leonina*, using acceleration data loggers. Deep Sea Res II 88–89: 14–22
Goldsworthy SD, Page B, Welling A, Chambellant M, Bradshaw CJA (2010) Selection of diving strategy by Antarctic fur seals depends on where and when foraging takes place. Mar Ecol Prog Ser 409:255–266
Good PI (2005) Permutation, parametric, and bootstrap tests of hypotheses, 3rd edn. Springer-Verlag, New York, NY
Guinet C, Dubroca L, Lea MA, Goldsworthy S and others (2001) Spatial distribution of foraging in female Antarctic fur seals *Arctocephalus gazella* in relation to oceanographic variables: a scale-dependent approach using geographic information systems. Mar Ecol Prog Ser 219:251–264
Guinet C, Xing X, Walker E, Monestiez P and others (2013) Calibration procedures and first dataset of Southern Ocean chlorophyll *a* profiles collected by elephant seals equipped with a newly developed CTD-fluorescence tags. Earth Syst Sci Data 5:15–29
Guinet C, Vacquié-Garcia J, Picard B, Bessigneul G and others (2014) Southern elephant seal foraging success in relation to temperature and light conditions: insight into prey distribution. Mar Ecol Prog Ser 499:285–301
Heerah K, Hindell M, Guinet C, Charrassin JB (2014) A new method to quantify within dive foraging behaviour in marine predators. PLOS ONE 9:e99329
Henson SA, Dunne JP, Sarmiento JL (2009) Decadal variability in North Atlantic phytoplankton blooms. J Geophys Res 114:C04013
Holm-Hansen O, Hewes CD (2004) Deep chlorophyll-*a* maxima (DCMs) in Antarctic waters. I. Relationships between DCMs and the physical, chemical, and optical conditions in the upper water column. Polar Biol 27:699–710
Houston AI, McNamara JM (1985) A general theory of central place foraging for single-prey loaders. Theor Popul Biol 28:233–262
Huisman J, Pham Thi NN, Karl DM, Sommeijer B (2006) Reduced mixing generates oscillations and chaos in the oceanic deep chlorophyll maximum. Nature 439:322–325

Jaquet N, Whitehead H (1996) Scale-dependent correlation of sperm whale distribution with environmental features and productivity in the South Pacific. Mar Ecol Prog Ser 135:1–9

Jaud T, Dragon AC, Garcia JV, Guinet C (2012) Relationship between chlorophyll a concentration, light attenuation and diving depth of the southern elephant seal *Mirounga leonina*. PLOS ONE 7:e47444

Jouandet MP, Trull TW, Guidi L, Picheral M, Ebersbach F, Stemmann L, Blain S (2011) Optical imaging of mesopelagic particles indicates deep carbon flux beneath a natural iron-fertilized bloom in the Southern Ocean. Limnol Oceanogr 56:1130–1140

Lea MA, Cherel Y, Guinet C, Nichols PD (2002a) Antarctic fur seals foraging in the Polar Frontal Zone: inter-annual shifts in diet as shown from fecal and fatty acid analyses. Mar Ecol Prog Ser 245:281–297

Lea MA, Hindell M, Guinet C, Goldsworthy SD (2002b) Variability in the diving activity of Antarctic fur seals, *Arctocephalus gazella*, at Iles Kerguelen. Polar Biol 25: 269–279

Lee Z, Marra J, Perry MJ, Kahru M (2015) Estimating oceanic primary productivity from ocean color remote sensing: a strategic assessment. J Mar Syst 149:50–59

Liu SH, Sun S, Han BP (2003) Diel vertical migration of zooplankton following optimal food intake under predation. J Plankton Res 25:1069–1077

Loots C, Koubbi P, Duhamel G (2007) Habitat modelling of *Electrona antarctica* (Myctophidae, Pisces) in Kerguelen by generalized additive models and geographic information systems. Polar Biol 30:951–959

Lopez R, Malardé JP, Royer F, Gaspar P (2014) Improving Argos Doppler location using multiple-model Kalman filtering. IEEE Trans Geosci Remote Sens 52:4744–4755

McConnell BJ, Chambers C, Fedak MA (1992) Foraging ecology of southern elephant seals in relation to the bathymetry and productivity of the Southern Ocean. Antarct Sci 4:393–398

McIntyre T, de Bruyn PJN, Ansorge IJ, Bester MN, Bornemann H, Plötz J, Tosh CA (2010) A lifetime at depth: vertical distribution of southern elephant seals in the water column. Polar Biol 33:1037–1048

Mongin MM, Abraham ER, Trull TW (2009) Winter advection of iron can explain the summer phytoplankton bloom that extends 1000 km downstream of the Kerguelen Plateau in the Southern Ocean. J Mar Res 67: 225–237

Moore JK, Abbott MR (2000) Phytoplankton chlorophyll distributions and primary production in the Southern Ocean. J Geophys Res Oceans 105:28709–28722

Morel A, Maritorena S (2001) Bio-optical properties of oceanic waters: a reappraisal. J Geophys Res Oceans 106: 7163–7180

Morel A, Prieur L (1977) Analysis of variations in ocean color. Limnol Oceanogr 22:709–722

O'Toole MD, Lea MA, Guinet C, Hindell MA (2014) Estimating trans-seasonal variability in water column biomass for a highly migratory, deep diving predator. PLOS ONE 9:e113171

Orians GH, Pearson NE (1979) On the ecology of central place foraging. In: Horn DJ, Mitchell RD, Stairs GR (eds) Analysis of ecological systems. The Ohio State University Press, Columbus, OH, p 155–177

Péron C, Weimerskirch H, Bost CA (2012) Projected poleward shift of king penguins' (*Aptenodytes patagonicus*) foraging range at the Crozet Islands, southern Indian Ocean. Proc Biol Sci 279:2515–2523

Pinheiro J, Bates D, Debroy S, Sarkar D, R Development Core Team (2015) nlme: Linear and nonlinear mixed effects models. R Package version 3:1–96. https://cran.r-project.org/web/packages/nlme/

Polovina J, Uchida I, Balazs G, Howell EA, Parker D, Dutton P (2006) The Kuroshio Extension Bifurcation Region: a pelagic hotspot for juvenile loggerhead sea turtles. Deep Sea Res II 53:326–339

R Development Core Team (2016) R: a language and environment for statistical computing. R Foundation for Statistical Computing, Vienna

Robins DB, Harris RP, Bedo AW, Fernandez E, Fileman TW, Harbour DS, Head RN (1995) The relationship between suspended particulate material, phytoplankton and zooplankton during the retreat of the marginal ice zone in the Bellingshausen Sea. Deep Sea Res II 42:1137–1158

Russell RW, Hunt GL, Coyle KO, Cooney RT (1992) Foraging in a fractal environment: spatial patterns in a marine predator-prey system. Landsc Ecol 7:195–209

Sala JE, Quintana F, Wilson RP, Dignani J, Lewis MN, Campagna C (2011) Pitching a new angle on elephant seal dive patterns. Polar Biol 34:1197–1209

Scheffer A, Trathan PN, Edmonston JG, Bost CA (2016) Combined influence of meso-scale circulation and bathymetry on the foraging behaviour of a diving predator, the king penguin (*Aptenodytes patagonicus*). Prog Oceanogr 141:1–16

Sokolov S, Rintoul SR (2007) On the relationship between fronts of the Antarctic Circumpolar Current and surface chlorophyll concentrations in the Southern Ocean. J Geophys Res 112:C07030

Sumner MD, Wotherspoon S, R Development Core Team (2013) tripEstimation: metropolis sampler and supporting functions for estimating animal movement from archival tags and satellite fixes, version 0.0-41. www.r-pkg.org/pkg/tripEstimation

Teo SLH, Kudela RM, Rais A, Perle C, Costa DP, Block BA (2009) Estimating chlorophyll profiles from electronic tags deployed on pelagic animals. Aquat Biol 5:195–207

Thums M, Bradshaw CJA, Hindell MA (2011) In situ measures of foraging success and prey encounter reveal marine habitat-dependent search strategies. Ecology 92: 1258–1270

Venrick EL (1993) Phytoplankton seasonality in the central North Pacific: the endless summer reconsidered. Limnol Oceanogr 38:1135–1149

Viviant M, Trites AW, Rosen DAS, Monestiez P, Guinet C (2010) Prey capture attempts can be detected in Steller sea lions and other marine predators using accelerometers. Polar Biol 33:713–719

Ware DM, Thomson RE (2005) Bottom-up ecosystem trophic dynamics determine fish production in the Northeast Pacific. Science 308:1280–1284

Watanabe YY, Takahashi A (2013) Linking animal-borne video to accelerometers reveals prey capture variability. Proc Natl Acad Sci USA 110:2199–2204

Zuur AF, Ieno EN, Walker NJ, Saveliev AA, Smith GM (2011) Mixed effects models and extensions in ecology with R. Springer, New York, NY

Editorial responsibility: Keith Hobson, London, Ontario, Canada

Submitted: March 7, 2017; Accepted: August 20, 2017
Proofs received from author(s): October 4, 2017